

Indium–Vanadium Oxides Deposited by Radio Frequency Sputtering: New Thin Film Transparent Materials for Li-Insertion Electrochemical Devices

F. Artuso,^{*,†,‡} F. Decker,^{†,‡} A. Krasilnikova,[§] M. Liberatore,[†] A. Lourenco,^{||}
E. Masetti,[§] A. Pennisi,^{‡,⊥} and F. Simone^{‡,⊥}

Chemistry Department, University of Roma "La Sapienza", I-00185 Roma, Italy,
ENEA-Casaccia, Thin Films Laboratory, Via Anguillarese, 00060 Roma, Italy, UNICAMP/
IFGW/DFA, CP 6165, CEP 13084-970, Campinas, SP, Brazil, Physics Department,
University of Catania, Corso Italia 57, 95129 Catania, Italy, and
Istituto Nazionale di Fisica della Materia, INFN

Received June 11, 2001. Revised Manuscript Received November 4, 2001

Thin films of mixed In/V oxides have been obtained by reactive RF sputtering. Their optical and electrochemical performances have been investigated in order to determine their possible applications in electrochromic devices as optically passive ion-storage layers. The targets used have been made of In₂O₃ and V₂O₅ powders mixed in different In/V ratios in a reactive sputtering atmosphere. Cyclic voltammetry and chronopotentiometry studies of these films have been performed. The films demonstrate high ion-storage capacity retained even after 1000 cycles without any significant degradation. Lithium diffusion coefficients, calculated by the potentiostatic intermittent titration technique (PITT), range around 10⁻¹³ cm² s⁻¹. The optical measurements, taken in the UV–vis–NIR transmittance and reflectance modes, have demonstrated that films are electrochromic, but the presence of In enhances their transparency and optical passiveness. The photometric spectra evaluation by a computer fitting shows that the refractive index is lower for films with higher In content. This result is in good agreement with Rutherford backscattering spectroscopy (RBS) measurements. The material structure has been discussed on the basis of the above results, as a function of the measured thin film composition, and is corroborated by preliminary results of XPS surface analysis.

1. Introduction

The class of orthovanadates (RVO₄) has received considerable interest as materials for electrochemical devices owing to their excellent properties as intercalation hosts for lithium ions. They have been recently proposed as potential anodes for lithium ion batteries¹ and also, in the form of thin films, as optically passive counter electrodes in electrochromic devices (ECD) with variable light transmission ("smart windows").^{2,3} As has been demonstrated in many works, metal/vanadium mixed oxides have favorable properties when used as charge storage electrodes in tandem with WO₃, the best coloring film for EC windows applications.⁴ In fact they have high transmittance both in the pristine and

lithium-intercalated states, associated to a considerable ion-storage capacity typical for the parent V oxides.

However, the vanadates investigated up to now do not obey the requirements of the ideal optically passive counter electrode for ECD based on WO₃. The properties that still have to be improved in the mixed vanadates are the charge capacity, to balance the ionic charge required by WO₃, and the weak optical absorption in the red due to the presence of the V₂O₅ parent oxide.⁴ The kinetics of the charge insertion/extraction reaction must be increased to give a faster electrochromic response. Many attempts have been made to solve these problems by mixing V₂O₅ with different foreign ions (Nb, Cr, Fe, Ti, Zr, Ce, ...),^{2,5–7} and encouraging results have been recently achieved with cerium–vanadium and nickel–vanadium mixed oxides.^{8–10} We were aiming at

* Corresponding author. Email: artuso@uniroma1.it.

† University of Roma "La Sapienza".

‡ Istituto Nazionale di Fisica della Materia.

§ ENEA-Casaccia.

|| UNICAMP/IFGW/DFA.

⊥ University of Catania.

(1) Denis, S.; Baudrin, E.; Touboul, M.; Tarascon, J.-M. *J. Electrochem. Soc.* **1997**, *144* (No. 12), 4099.

(2) Opara Krasovec, U.; Orel, B.; Reisfeld, R. *Electrochim. Solid-State Lett.* **1998**, *1*, 104.

(3) Artuso, F.; Picardi, G.; Decker, F.; Bonino, F.; Bencic, S.; Surca, A.; Opara Krasovec, U.; Orel, B. *Electrochim. Acta* **2001**, *46*, 2077–2084.

(4) Granqvist, C. G. *Handbook of Inorganic Electrochromic Materials*; Elsevier: Amsterdam, 1995.

(5) Surca, A.; Orel, B.; Drazic, B.; Decker, F.; Colombari, P. Submitted to *J. Sol-Gel Sci. Technol.*

(6) Cogan, S. F.; Rauh, R. D.; Nguyen, N. M.; Plante, T. D.; Westwood, J. D. *J. Electrochem. Soc.* **1993**, *140*, 112.

(7) Veszlei, M.; Kullman, L.; Azens, A.; Granqvist, C. G.; Hjørversson, B. *J. Appl. Phys.* **1997**, *81*, 2024.

(8) Picardi, G.; Varsano, F.; Decker, F.; Opara-Krasovec, U.; Surca, A.; Orel, B. *Electrochim. Acta* **1999**, *44*, 3157.

(9) Masetti, E.; Varsano, F.; Decker, F.; Krasilnikova, A. *Electrochim. Acta* **2001**, *46*, 2085–2090.

(10) Lourenco, A.; Masetti, E.; Decker, F. *Electrochim. Acta* **2001**, *46*, 2257–2262.

an ideal counter electrode that satisfies at the same time all requirements listed before we decided to study the electrochemical properties of InVO_4 , previously investigated by Denis et al.¹ for lithium battery electrodes.

Structural studies by Touboul et al.^{11,12} showed that InVO_4 belongs to the class of orthovanadates (RVO_4) and can crystallize both in an orthorhombic $Cmcm$ phase ($\text{InVO}_4\text{-III}$) when annealed at high temperature and in a metastable monoclinic low-temperature $C2/m$ phase ($\text{InVO}_4\text{-I}$). Both phases present a structure consisting of VO_4 tetrahedra sharing corners with InO_6 octahedra. This layered structure is particularly suitable, in principle, for insertion of lithium ions, as it is rich in channels.

The results of the works above showed that both amorphous and crystallized InVO_4 are interesting candidates as negative electrodes in lithium-ion rechargeable batteries, since they exhibit reversible capacities as large as 900 mAh/g. Amorphous $\text{InVO}_4 \cdot 2.3\text{H}_2\text{O}$ powders displayed a higher charge capacity than the orthorhombic and monoclinic phases, although they showed larger irreversible charge retention during the first cycles. Recently, InVO_4 was also studied in the form of a thin film by Orel et al.^{13,14} They prepared the films by sol–gel and heat treatment: the crystalline films, with a thickness up to 230 nm, displayed a considerable charge capacity of about 40 mC cm^{-2} . Their in-situ UV–vis spectroelectrochemical studies of amorphous and crystalline films showed, however, that the films have a cathodic coloration with a decrease in the photopic transmittance by 16% upon Li electrochemical insertion.

On the basis of our previous experience with CeVO_4 , obtained by sputtering and showing electrochemical behavior better than or at least comparable to the one of CeVO_4 synthesized by the sol–gel method,^{8,9} the RF sputtering technique has been chosen by us for indium vanadate film preparation. Our objective is to obtain thinner and more homogeneous films than the sol–gel ones, but with the same charge capacity, and to enhance the film optical transmittance and color neutrality exploiting the lower and more uniform thickness, proving that sputtering is suitable for such transparent intercalation electrodes. The preparation of the films, the electrochemical study of Li intercalation/deintercalation reactions, and the investigation of the optical and compositional properties of In/V films with different In contents and Li inserted charges are the subject of the present paper.

2. Experimental Section

Indium–vanadium mixed oxide thin films were deposited by radio frequency (RF) sputtering, using an apparatus reported in ref 15, from a single 15 cm diameter target made of In_2O_3 (CERAC) and V_2O_5 (CERAC) powders, finely mixed with three different In/V molar ratios, 1.0, 0.5, and 0.25 (samples In50, In33, and In20, respectively), and cold pressed. The film substrates were either B270 glass flats or indium tin

Table 1. Properties of Samples In50, In33, and In20^a

sample	l (nm)	d (g cm^{-3})	In/V	O/V	n_{633}	E_{gap} (eV)	V_{oc} (V vs Li)	T_{vis} (%)
In50	145	2.42	0.8	4	2.00	2.6	3.2	84.2
In33	135	2.74	0.5	4	2.07	2.4	3.46	82.3
In20	142	3.05	0.2	2.3	2.14	2.32	3.68	80.2

^a The density (d) and In/V and O/V ratios were evaluated with the RBS technique. The film thickness (l), the refractive index at 633 nm (n_{633}), and the photopic transmittance (T_{vis}) results were calculated from optical measurements. The values of T_{vis} are relative to the films as-deposited on glass. The electromotive force (V_{oc}) was measured on films as-grown assembled in a cell with lithium as reference and counter electrodes.

oxide (ITO) covered glass conductive substrates ($\sim 20 \Omega/\square$) in order to perform optical and/or spectroelectrochemical characterizations. The substrates were fixed on a cooled holder at about 5.0 cm distance from the target. The vacuum in the chamber before film deposition was 10^{-6} Torr, and the working pressure for sputtering was 30 mTorr. All samples were deposited by the reactive sputtering technique, using oxygen and argon partial pressures in the ratio 1:5. The applied RF power during the presputtering and sputtering process was always 200 W.

The deposited films were analyzed using various characterization techniques. Film thickness and optical parameters have been evaluated from spectrophotometric data.¹⁵ The film microstructure was analyzed by X-ray diffraction (XRD) while the atomic composition and film density were measured using Rutherford backscattering (RBS, see Table 1) and X-ray photoelectron spectroscopy (XPS).

Reflectance and transmittance spectra measurements have been taken with a Perkin-Elmer $\lambda 9$ spectrophotometer of the as-grown thin films deposited onto a B270 glass substrate in the UV–vis optical range (320–900 nm). Further transmittance and reflectance spectra were taken of samples deposited onto an ITO glass substrate, intercalated or deintercalated after a hundred cycles, washed in acetonitrile, and dried in a vacuum, to check their electrochromic behavior. The same samples were observed later under a commercial atomic force microscope (AFM), to check the sample morphology and its surface roughness.

The electrochemical intercalation/deintercalation process was accomplished either by cyclic voltammetry (at scan rates of 1, 10, and 20 mV s^{-1}) or by a galvanostatic technique (chronopotentiometry, under a constant current density of 10–50 $\mu\text{A cm}^{-2}$). Both techniques were confined to potentials between the limits of 4.5 and 1.0 V versus Li in a three-electrode cell, filled under argon in a glovebox with 1 M $\text{LiClO}_4/\text{EC:DMC}-1:1$ electrolyte. The electrode active area was 1 cm^2 , and lithium foils were used as the counter electrode and reference electrode. To measure the diffusion coefficient (D) of the lithium ions in this material, we used the potentiostatic intermittent titration technique (PITT).¹⁶

3. Results

3.1. Structural and Optical Characterization.

Three sets of thin films with different compositions of indium–vanadium oxides were prepared, in this work named as samples In50, In33, and In20, with corresponding In/V ratios (in the sputtered target) of 1.0, 0.5, and 0.25, and with thicknesses of 146, 135, and 142 nm, respectively.

XRD grazing angle incident beam measurements revealed that In–V thin films were completely amorphous, apart from the sample In50, where traces of a crystalline In_2O_3 phase appeared in XRD spectra. XPS

(11) Touboul, M.; Toledano, P. *Acta Crystallogr.* **1980**, *B36*, 240–245.

(12) Touboul, M.; Ingrain, D. *J. Less-Common Met.* **1980**, *55*, 62.

(13) Surca Vuk, A.; Opara Krasovec, U.; Orel, B.; Colomban, P. *J. Electrochem. Soc.* **2001**, *148*, H49–H60.

(14) Orel, B.; Surca Vuk, A.; Opara Krasovec, U.; Drazis, G. *Electrochim. Acta* **2001**, *46*, 2059–2068.

(15) Masetti, E.; Varsano, F.; Decker, F. *Electrochim. Acta* **1999**, *44*, 3117–3119.

(16) Levi, M. D.; Levi, E. A.; Aurbach, D. *J. Electroanal. Chem.* **1997**, *421*, 89–97.

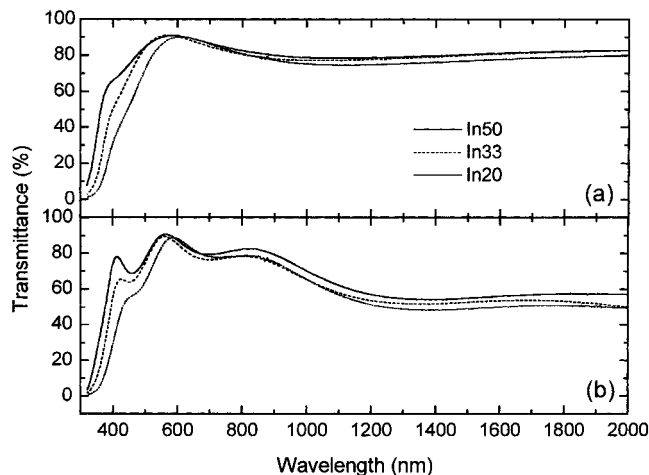


Figure 1. Spectral transmittance: (a) as-grown on glass; (b) as-grown on ITO/glass; (solid line) In50; (dash line) In33; (dot line) In20.

analysis performed on the as deposited films as well as on a standard of InVO_4 (orthorhombic phase) powder confirmed that the V/O and V/In ratios of In50 and In33 have values close to the ones of InVO_4 with a slight decrease of vanadium surface concentration. Moreover, the Auger parameter α' of vanadium 2p measured for In50 and In33 is very close to that of standard InVO_4 powder, whereas α' of In20 is closer to the one of V_2O_5 .¹⁷

The optical transmittance obtained by UV–vis spectrophotometric measurements (see Figure 1) was elaborated in terms of photopic transmittance (T_{vis}) according to the following formula:¹⁸

$$T_{\text{vis}} = \frac{\int_{\lambda=350\text{nm}}^{820\text{nm}} T(\lambda) R(\lambda) d\lambda}{\int_{\lambda=350\text{nm}}^{820\text{nm}} R(\lambda) d\lambda}$$

where $T(\lambda)$ represents the spectral transmittance of the sample and $R(\lambda)$ is the eye spectral response. The as-deposited thin films showed a yellowish coloration, more intense the higher the vanadium content. The variation in spectral transmittance as a function of the indium content for as-grown thin films can be seen in Figure 1a for films on B270 glass and in Figure 1b for films on glass/ITO conductive substrates. One can observe that the increase of indium concentration enhances the transmittance and depresses the strong absorption below 500 nm, typical for the vanadium pentoxide thin films.¹⁹ The photopic transmittance calculated for the samples In50, In33, and In20 on glass was 84.2%, 82.3%, and 80.2%, respectively. Measurements made on three similar samples deposited on glass + ITO resulted in T_{vis} equal to 79.9%, 76.6%, and 75.6%, respectively, associated with interference effects due to the underlying ITO layer. From the transmittance and reflectance spectra, the refractive index n , the extinction coefficient k of the films, and the film thickness were calculated using a fitting procedure.¹⁵ In general, the near-UV absorption in these mixed oxides is less pronounced than

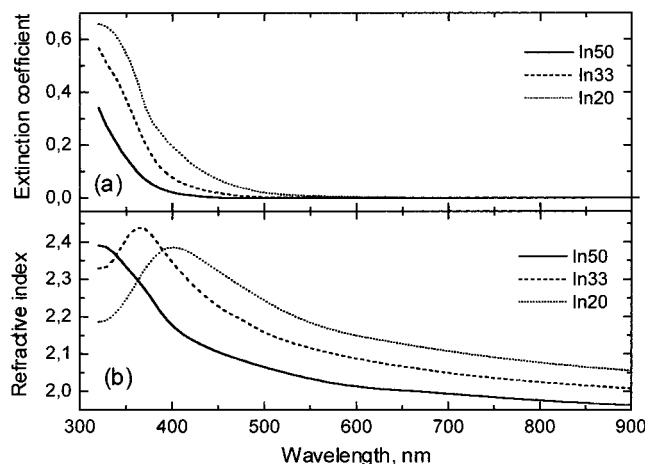


Figure 2. Dispersion of extinction coefficient (a) and refractive index (b); (solid line) In50; (dash line) In33; (dot line) In20.

that in pure V_2O_5 , according to the lower vanadium concentration in In–V mixed oxides. As shown in Figure 2a, the k values for sample In20, deposited with a smaller In/V ratio (0.25), rise from 500 nm toward shorter wavelengths, accounting for the yellowish coloration of the samples. This absorption moves away toward the UV for samples In50 and In33. This result is in agreement with data from other authors that have reported fundamental absorption edges in the range 460–550 nm for V_2O_5 thin films.^{19,20} Figure 2b shows the refractive index dispersion: n values were lower (2.0, 2.07, and 2.14 for samples In50, In33, and In20, respectively, at 633 nm) than those for pure V_2O_5 ($n_{633} = 2.3$).⁴ This result is in agreement with the density d obtained by RBS (in Table 1). In fact, with the increase of the vanadium concentration, the samples showed an increase both in d and in n . Furthermore, the RBS data proved that the films maintained very similar In/V ratios as in the target. The density (d) determined by this method was 2.42, 2.74, and 3.05 g cm^{-2} for In50, In33, and In20, respectively. These d values, lower than the ones calculated for the parent In_2O_3 ($d = 7.18 \text{ g cm}^{-3}$) and V_2O_5 ($d = 3.337 \text{ g cm}^{-3}$) oxides, are also quite different from the density reported for the orthorhombic crystalline stable InVO_4 -III phase (4.7 g cm^{-3}).¹¹

The band gap for the thin films has been evaluated by extrapolation of the linear portion of the plots $(\alpha h\nu)^{1/\eta}$ versus the photon energy $h\nu$, where $\eta = 2$, assuming that indium–vanadium mixed oxide thin films have a fundamental absorption edge of indirect type. The calculated band gap energy was $E_g = 2.6, 2.4, \text{ and } 2.32 \text{ eV}$ for samples In50, In33, and In20. These band gaps are all larger than 2.2 eV, which is the energy gap reported in the literature for pure V_2O_5 films,⁴ and smaller than 2.8 eV, which is the indirect band gap of In_2O_3 .²¹ This can be related to the presence of indium ions in the structure of the V_2O_5 ^{22,23} material or to the presence of a new indium vanadate phase, as discussed in the next section.

(20) Kenny, N.; Kannewurf, C. R.; Whitmore, D. H. *J. Phys. Chem. Solids* **1966**, *27*, 1237L.

(21) Schumacher, C.; Mamiche-Afara, S.; Dignam, M. J. *J. Electrochem. Soc.* **1986**, *716–728*.

(22) Moshfegh, A. Z.; Ignatiev, A. *Thin Solid Films* **1991**, *198*, 251.

(23) Benmoussa, M.; Ibnouelghazi, E.; Bennouna, A.; Ameziene, E. *L. Thin Solid Films* **1995**, *256*, 22–28.

(17) Zanoni, R.; Salvi, A. Private communication.

(18) Surca Vuk, A.; Orel, B.; Opara Krasovec, U.; Lavrencic Stangar, U.; Drazic, G. *J. Electrochem. Soc.* **2001**, *147*, 2358–2370.

(19) Cogan, S. F.; Nyugen, N. M.; Perrotti, S. J.; Rauh, R. D. *J. Appl. Phys.* **1989**, *66*, 1333.

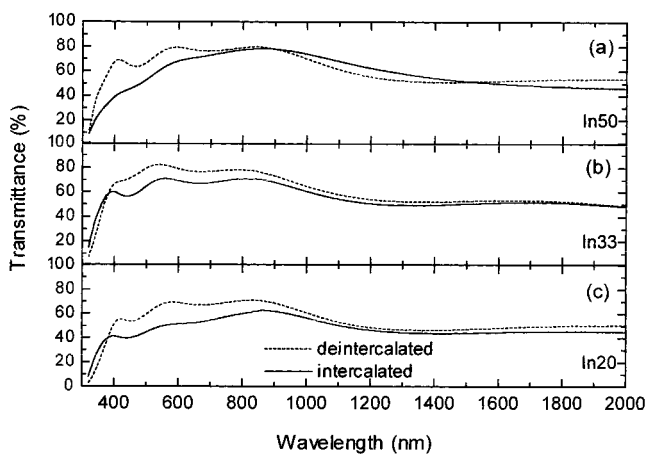


Figure 3. Spectral transmittance of fully deintercalated (dot line) and intercalated (solid line) films after a hundred cycles. Samples In50 (a), In33 (b), and In20 (c).

The ex-situ UV–vis optical responses of indium–vanadium mixed oxides, both fully deintercalated and intercalated after a hundred cycles, are shown in Figure 3. All samples presented low electrochromic activity: sample In50 had a cathodic behavior from 200 up to 900 nm and a mixed anodic/cathodic electrochromism in the NIR; samples In33 and In20 showed only a cathodic behavior between 400 and 2000 nm, possibly due to the polaron hopping²⁴ also observed in V_2O_5 films. Samples In20 and In33 were bleaching with intercalation between 320 and 400 nm, as expected from optical transitions in the partially filled bands (i.e. from band gap widening). The photopic transmittance, calculated by ex-situ measurements, was 74.6%, 77.1%, and 75.6% (deintercalated) and 62.7%, 66.0%, and 49.0% (intercalated), for samples In50, In33, and In20. After 1000 cycles, the transmittance spectra showed only small changes, confirming the high stability of such films. It is remarkable that In50, which in the as-deposited state showed the highest transmittance, became less transparent than In33 with cycling, when deintercalated. As will be shown in the next section, this coloring associated with cycling can be explained with the high, irreversible charge retention of sample In50 during the first cycles.

Results of photopic transmittance on $InVO_4$ films made by the sol–gel technique where obtained by Orel et al.^{13,14} From in-situ spectroelectrochemical UV–vis analysis on films made by a single dipping cycle and heat-treated at 500 °C, they obtained a photopic transmittance above 87.1% for the as-deposited and discharged samples, while on the charged films the photopic transmittance dropped to 72.2%. To compare our ex-situ measurements (in air) with the T_{vis} values obtained with in-situ experiments (in the cell) performed by Orel et al., we should take into account the reflections at the air/sample interfaces, in comparison with the reflections of the sample dipped in the electrolyte. Considering that the light reflected in air by the glass substrate is 4%, and that reflected by the In/V film ($n_{av} = 2.07$) is about 12% of the incident radiation (while in propylene carbonate it is only 1.4%), the values of T_{vis} evaluated for our In/V films seem to be quite similar to the ones obtained by Orel.

(24) Talledo, A.; Granqvist, C. G. *J. Appl. Phys.* **1995**, *77*, 4655.

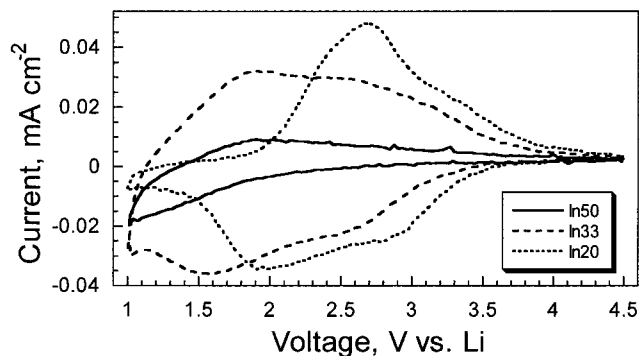


Figure 4. Cyclic voltammeteries at 1 mV s^{-1} for samples In50 (solid line), In33 (dash line), and In20 (dot line) after 10 cycles.

3.2. Electrochemical Characterization. The lithium insertion reaction was investigated by cyclic voltammetry (CV), chronopotentiometry, and the potentiostatic intermittent titration technique (PITT). The electromotive force (V_{OC}) of samples In50, In33, and In20 was 3.2, 3.46, and 3.68 V versus Li, immediately after cell assembling. These results are reasonable, as the V_{OC} values reported in the literature for the parents V_2O_5 and In_2O_3 made by sputtering were 3.6–3.7 V⁴ and 2.8–3.1 V.²⁵ Cyclic voltammograms of In–V mixed oxide thin film electrodes after 10 cycles of Li ion intercalation and deintercalation are reported in Figure 4. Different voltammetric profiles appeared for different indium contents. Sample In20 presented an electrochemically active region between 1.5 and 3.7 V, one large anodic peak at 2.7 V, and two not well-defined cathodic peaks at 2.0 and 2.9 V. This cyclic voltammogram was quite similar to the one observed in nickel–vanadium mixed oxides thin films.¹⁰ The electrochemically active region extended further down to 1.0 V for the sample In33. The reversibility of lithium ion insertion and extraction after 10 cycles was good for films In33 and In20. However, the sample In50 presented a very low current density and irreversible Li insertion. All In–V mixed oxide thin films with high indium content showed a peculiar electrochemical feature that was also observed and experienced in some intercalation compound thin films as NiO_x ,²⁶ In_2O_3 .²⁷ These materials needed an initial “activation” process; that is, an initial injection of Li ions was necessary to activate the host structure and to trigger fast and reversible insertion and deinsertion reactions. This mechanism will be discussed in the next section.

The activation process can be accomplished using different electrochemical techniques. By CV it was possible, keeping the potential sweep window between 1 and 4.5 V versus Li at the scan rate of 1 mV s^{-1} , to observe considerable changes in the shape and characteristics of the current–voltage curves. In the first few cycles with sample In50 the cathodic and anodic currents were very low and the corresponding intercalated charge was only 2.6 mC cm^{-2} (Figure 5). During the first cycles an irreversible process occurred (the permanent uptake of Li ions) that caused a change in the sample

(25) Golden, S. J.; Steele, B. C. H. *Solid State Ionics* **1987**, *28–30*, 1733–1737.

(26) Decker, F.; Passerini, S.; Pileggi, R.; Scrosati, B. *Electrochim. Acta* **1992**, *37* (No. 6), 1033–1038.

(27) Hamberg, I.; Granqvist, C. G. *J. Appl. Phys.* **1986**, *60* (11), R123.

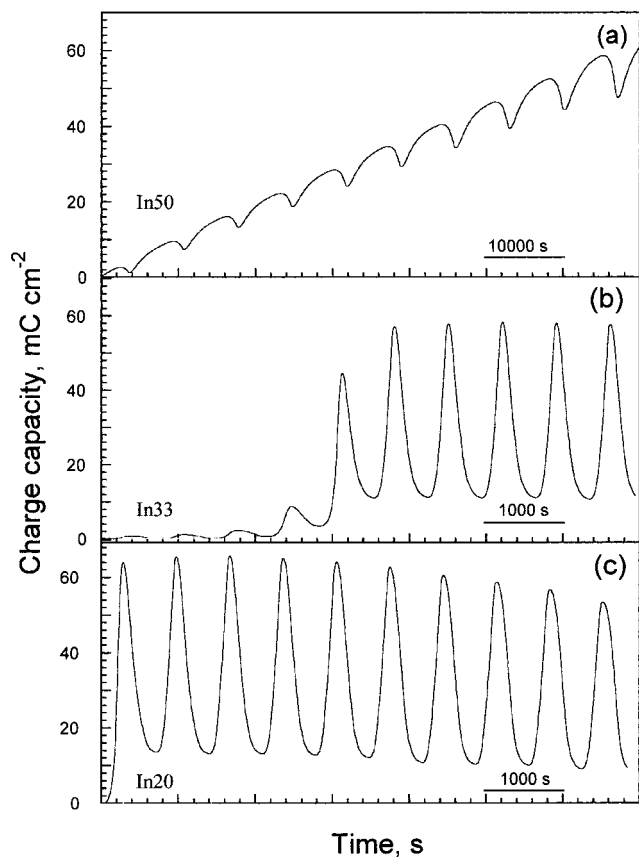


Figure 5. Charge capacity as a function of time during the first 10 cycles of cyclic voltammetry: the scan rate is 1 mV s^{-1} for sample In50 (a) and 10 mV s^{-1} for samples In33 (b) and In20 (c).

electrochemical and optical activities. The large charge retention during the initial cycles and a slow and progressive increase of charge capacity were displayed by sample In50 (Figure 5a). Only after scanning In50 for 20 cycles at a 1 mV s^{-1} rate did the charge/discharge process become reversible and the charge capacity achieve a steady value. After about 100 cycles the charge capacity stabilized at 40 mC cm^{-2} , remaining stable even after 1000 cycles. The shape of the CV curve of our In50 electrode closely resembles the voltammogram of sol-gel InVO_4 obtained by Orel et al.^{13,14} after a mild thermal treatment at $300 \text{ }^\circ\text{C}$.

Sample In33 needed also an activation process, achieving a steady-state voltammogram only after a few cycles at 10 mV s^{-1} (Figure 5b). 20% of the charge was retained in five insertion/extraction cycles. Sample In20 had a different behavior: only in the first insertion step did it retain 20% of the charge, and in the subsequent cycles it suffered a small and gradual loss of capacity. Denis et al.¹ observed a similar behavior for low-temperature amorphous In vanadates ($\text{InVO}_4 \cdot 2.3\text{H}_2\text{O}$) which showed during the first cycle an irreversible charge retention much larger than 20%.

Typical galvanostatic Li insertion/extraction curves for the samples In50, In33, and In20 after a hundred cycles are shown in Figure 6a. The current density used for cell charging/discharging was $\pm 10 \text{ } \mu\text{A cm}^{-2}$; the charge capacity was about 40 mC cm^{-2} for all films. In contrast with the discharge curves of crystalline V_2O_5 ,²⁸ no defined voltage plateau and sharp steps were ob-

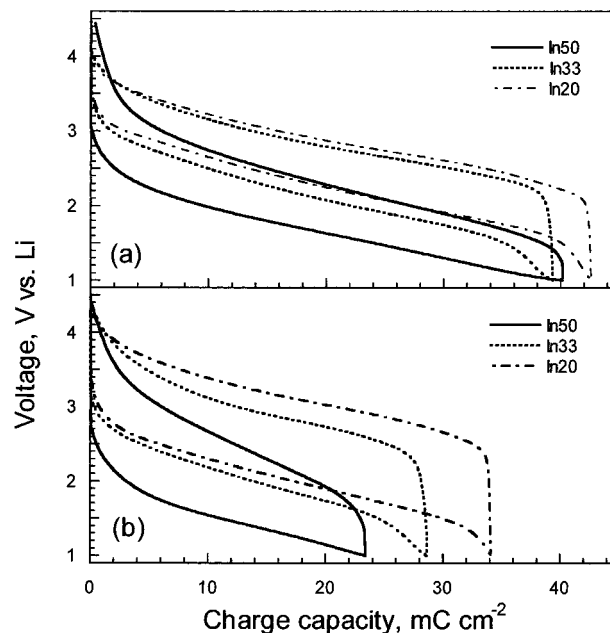


Figure 6. Chronopotentiometry at $I = \pm 10 \text{ } \mu\text{A cm}^{-2}$ (a) and $I = \pm 50 \text{ } \mu\text{A cm}^{-2}$ (b) for samples In50 (solid line), In33 (dash line), and In20 (dot line).

served under galvanostatic discharge, which confirms the amorphous structure²⁹ of the sputtered In-V mixed oxide films. The specific capacity of the oxides decreased according to the value of the applied current density, as shown in Figure 6b. The chronopotentiometric curves of the same three samples In50, In33, and In20 at $\pm 50 \text{ } \mu\text{A cm}^{-2}$ after 100 cycles indicated that the samples had different charge capacities, while with a current density of $\pm 10 \text{ } \mu\text{A cm}^{-2}$ all showed almost the same capacity independently of the In concentration in the films.

Since at higher current density the capacity is dependent on composition, this may be due to the different ionic diffusion properties of the three samples. Sample In50 also showed a larger hysteresis in the E versus Q curves recorded during the charge and discharge processes at constant current. These results were correlated to measurements of ionic diffusion coefficients (D) obtained by the potentiostatic intermittent titration technique (PITT), performed in the potential range 2.5–1.4 V after a hundred CV cycles. The approach already used by Levi et al.,³⁰ in which a plateau in the $It^{1/2}$ versus $\log t$ plot represents the Cottrell region, was used to calculate the D values from the equation

$$It^{1/2} = \frac{D_1^{1/2} \Delta Q}{l\tau^{1/2}}$$

where ΔQ is the amount of charge injected into the electrode during the potential step and l is the film thickness. In our experiments potential steps of 50 mV with a duration of 600 s were applied.

In Figure 7 the diffusion coefficients (D) for Li ion inside the oxide films are plotted as a function of

(28) Talledo, A.; Andersson, A. M.; Granqvist, C. G. *J. Appl. Phys.* **1991**, *69*, 3261–3265.

(29) Passerini, S.; Scaramino, J.; Scrosati, B.; Zane, D.; Decker, F. *J. Appl. Electrochem.* **1993**, *23*, 1187–1195.

(30) Levi, M. D.; Levi, E. A.; Aurbach, D. *J. Electroanal. Chem.* **1997**, *421*, 89.

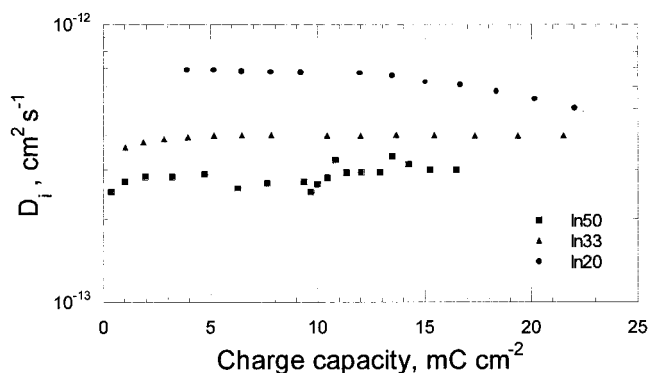


Figure 7. Ionic diffusion coefficient (D_i) as a function of charge capacity for samples In50, In33, and In20.

inserted charge. As was expected, sample In50 had a lower value of D_i than sample In20, and sample In33 showed an intermediate D_i . All D_i values were between 10^{-12} and 10^{-13} $\text{cm}^2 \text{s}^{-1}$, similarly to what was reported in the literature for other vanadium compounds.^{8,31}

Concerning the electrochemical characterization, it is important to point out that our samples were analyzed in a wide potential window between 1 and 4.5 V. These potential limits are out of the so-called “safe region” for several vanadium oxide electrodes. In fact, V_2O_5 crystalline thin films cycled between 4.5 and 1.5 V exhibit a much larger capacity fade than those cycled between 4.1 and 2.0 V.³² However, for amorphous films, like our samples, it was proven to be possible to cycle the electrodes down to 1.5 or even 1.0 V without severe capacity losses.

4. Discussion

According to XRD analysis, all films were amorphous. We can infer, however, the short-range order in the In/V films from XPS and RBS data (Table 1) and try to correlate the electrochemical and optical behavior of our thin films to the properties of well-defined crystalline oxide electrodes reported in the literature. The XPS analysis performed on the as deposited films suggested that the chemical bonds in In50 and In33 are similar to those of standard InVO_4 powder, whereas for In20 there is a similarity in the spectra both with V_2O_5 and with InVO_4 . It can be supposed, therefore, that in our films the In^{3+} and V^{5+} ions contribute to a short-range structure closely similar to that of indium vanadate, consisting of VO_4 tetrahedra and of InO_6 octahedra.

Only with the measured composition of the In20 sample (O/V atomic ratio of 2.3, from RBS data), could the In^{3+} ions be viewed as dopants of V_2O_5 , similarly to what was reported by Coustier et al.³³ for aerogel vanadium oxides heavily doped with Ag^+ and Cu^{2+} ions. In addition, the optical and electrochemical results on In20 are consistent with the above hypothesis: V_{oc} and CV are similar to those of pure, amorphous V_2O_5 ,³⁴

whereas the band gap energy, only slightly larger than that of V_2O_5 , is the main indication for the indium doping.

In the case of sample In33, the presence of indium vanadate together with other vanadium oxides (suggested by XPS data) could be indicated also by the electrode activation and by the Li^+ ion retention during the first five cycles. In fact, the high Li uptake of amorphous indium vanadate materials has been reported by Denis et al.¹ and justified in terms of a large BET surface area, being catalytic toward the irreversible capacity loss process or simply adsorbing more water and leading to an irreversible reaction with Li^+ with formation of metallic Li. In sample In50 the quantity of InVO_4 should be larger and consequently the amount of Li ion retention is larger. In our case, differently from that of Denis, this irreversible process requires several cycles and does not occur only in the first step. This is probably due to the narrower electrochemical potential window used by us (from 1 to 4.5 V) deliberately, to avoid large mechanical stresses in the sample with the danger of film disruption or detachment from its glass substrate. For all samples the Li insertion/removal process became completely reversible after the system was activated toward further Li^+ intercalation and no mechanical damage was observed. Once activated, sample In50 displayed a good electrochemical performance, getting a stable charge capacity of 40 mC cm^{-2} , which corresponds to over 300 mAh/g. Its charge capacity fading was the lowest among all the samples tested, being of only 0.003% per cycle of the reversibly inserted charge, after more than 1000 cycles.

These data can be interpreted in terms of a higher porosity of sample In50. This decrease of sample density (by RBS results) and refractive index (see Figure 2b), observed for increasing In content in our films, would not fit well with a structural model considering two distinct V_2O_5 and In_2O_3 phases, because the In_2O_3 phase is the one with the highest density and refractivity, and with the lowest Li intercalation activity. The presence of In^{3+} , with an ionic radius much larger than that of V^{5+} ($r_{\text{In}^{3+}} = 0.81 \text{ \AA}$; $r_{\text{V}^{5+}} = 0.59 \text{ \AA}$), creates an open-framework structure, mainly consisting of orthovanadate InVO_4 units, with a large number of noncoordinated oxygen atoms, to which Li ions can be bound. This model is consistent with the results obtained by the electrochemical characterization and can account both for the permanent Li uptake, dependent on the In/V ratio in the different films, and for the need of an activation process, due to the larger energy needed to remove an inserted Li ion from such an open framework structure.

5. Conclusions

The optical and electrochemical properties of In/V mixed oxide thin films made by RF sputtering have been investigated in order to elucidate whether these films fulfill the characteristics of suitable transparent and passive counter electrodes for ECD applications. Our studies have shown that electrochemical and optical performances of In/V films were dependent on the indium content in the oxide matrix. XRD spectra have revealed that films were amorphous. XPS analyses suggested the presence of the InVO_4 compound in the

(31) Hayashibara, M.; Euchi, M.; Miura, T.; Kishi, T. *Solid State Ionics* **1997**, *98*, 119–125.

(32) Zhang, J.-G.; McGraw, J. M.; Turner, J.; Gingley, D. J. *Electrochem. Soc.* **1997**, *144*, 1630.

(33) Coustier, F.; Hill, J.; Owens, B. B.; Passerini, S.; Smyrl, W. H. *J. Electrochem. Soc.* **1999**, *146* (4), 1355–1360.

(34) Lourenco, A.; Gorenstein, A.; Passerini, S.; Smyrl, W. H.; Fantini, M. C. A.; Tabacniks, M. H. *J. Electrochem. Soc.* **1998**, *145*, 706.

films. The In–V oxide film density, refractive index, and absorption coefficient decreased with the increase of indium content. After electrode activation, however, the permanent Li uptake was responsible for some additional optical absorption in the visible. The cyclic voltammetry and galvanostatic measurements have shown that sputtered In/V films may exhibit good ion-storage capacities of more than 40 mC cm^{-2} , for film only 150 nm thick. This charge capacity, after an initial activation process, is quite stable even after extensive charge/discharge cycling. The solid-state diffusion coefficient of Li in the films is in the range $10^{-13} \text{ cm}^2 \text{ s}^{-1}$.

Although it has been shown that sputtered In/V samples are transparent electrodes, with a good charge capacity, the optical passivity of the films is not yet ideal for ECD applications. The weak cathodic electrochromism of such films (sample In33 still presents 11.1% of the photopic transmittance variation), which is more evident in the blue region, may limit the

industrial applications for smart windows. The large charge capacity and the high value of the discharge voltage during intercalation, detected under chronopotentiometric measurements, suggest that a further utilization of these materials can be as a cathode in rechargeable thin film microbatteries.

Acknowledgment. This work has been funded by FAPESP, Brazil, Proc. No. 99/07138-9; the Consiglio Nazionale Ricerche—Project MSTA2-contract PF34, ENEA, Casaccia, Italy; and MURST—cofinanziamento 1999–2001. The authors would like to acknowledge Dr. R. Ceccato of University of Trento for XRD analysis, and Dr. R. Zanoni for XPS analysis. The authors are grateful to Mr. V. Conelli for helpful technical assistance during RBS analysis, and to Prof. M. Touboul for providing the InVO_4 powders used as standards.

CM010558L